A Novel Spectral-Efficient Resource Allocation Approach for NOMA-Based Full-Duplex Systems

Hieu V. Nguyen[1], Van-Dinh Nguyen[1], Octavia A. Dobre[2],
Diep N. Nguyen[3], Eryk Dutkiewicz[3], and Oh-Soon Shin[1]

[1]School of Electronic Engineering & Department of ICMC Convergence Technology, Soongsil University, Korea
[2]Faculty of Engineering and Applied Science, Memorial University, St. John's, NL, Canada
[3]Faculty of Engineering and Information Technology, University of Technology Sydney, Sydney, NSW 2007, Australia

Abstract—This paper investigates the coexistence of non-orthogonal multiple access (NOMA) and full-duplex (FD), where the NOMA successive interference cancellation technique is applied simultaneously to both uplink (UL) and downlink (DL) transmissions in the same time-frequency resource block. Specifically, we jointly optimize the user association (UA) and power control to maximize the overall sum rate, subject to user-specific quality-of-service and total transmit power constraints. To be spectrally-efficient, we introduce the tensor model to optimize the UL users' decoding order and the DL users' clustering, which results in a mixed-integer non-convex problem. For solving this problem, we first relax the binary variables to be continuous, and then propose a low-complexity design based on the combination of the inner convex approximation framework and the penalty method. Numerical results show that the proposed algorithm significantly outperforms the conventional FD-based schemes, FD-NOMA and its half-duplex counterpart with random UA.

Index Terms—Full-duplex radios, non-convex programming, non-orthogonal multiple access, self-interference, spectral efficiency, successive interference cancellation, user clustering.

I. INTRODUCTION

For the next generation wireless system, improving the spectral efficiency (SE) plays a pivotal role in meeting the exponential demand of mobile data and new services, especially over the limited radio spectrum [1]. To that end, non-orthogonal multiple access (NOMA) [2], [3] and in-band full-duplex communications are amongst the most promising solutions. Unlike conventional multiple access methods that separate concurrent transmissions onto different orthogonal dimensions (e.g., in code like CDMA, in time or frequency like TDMA or FDMA), NOMA allows multiple transmissions to coexist. Also to improve the SE, thanks to the latest advances in self-interference suppression, the in-band full-duplex (FD) radios can now transmit and receive simultaneously on the same frequency, even using the same antenna array or RF-chains. Theoretically, FD can double the SE of a wireless link over its half-duplex (HD) counterparts [4].

The coexistence of NOMA and FD has recently received paramount interest. The authors of [5], [6] focus on mitigating the network interference. In [7]–[9], the successive interference cancellation (SIC) technique was adopted for the UL reception in FD systems in which only the random decoding order with respect to (w.r.t.) UL users' indices was considered. An optimal user pairing in NOMA network was investigated in [10], but merely applied to the DL transmission. Additionally, a joint power and subcarrier allocation scheme to enhance the throughput of users was investigated in [11]. Further,

the authors in [5] showed that FD-NOMA can improve the achievable rate, while a joint NOMA beamforming and user scheduling in FD systems was also reported in [12]. It is worth noting that most of the above work simply adopts the random schemes for both UL and/or DL transmission. As such, this work aims to establish framework that optimizes DL user clustering as well as UL users' decoding order to maximize the total sum rate (SR).

To that end, we formulate a SR maximization problem for a FD-NOMA multiuser MISO (MU-MISO) system, subject to minimum data rate constraints for each user. Our formulation explicitly considers the effects of user association (UA) in both DL and UL channels. For the UL reception, we adopt the SIC technique that results in a permutation problem to optimize the UL users' decoding order. For the DL transmission, a promising approach is to divide DL users into multiple clusters with different channel conditions by introducing a tensor of binary numbers. NOMA is then implemented within each cluster. The resulting optimization problem is a mixed-integer non-convex programming, which often requires exponential time find its globally optimal solution. To tackle it, we propose novel transformations using on the inner convex approximation (ICA) framework and penalty function (PF) method. Numerical results are provided to demonstrate the convergence of the proposed algorithm and the achieved SR gains of the proposed FD-NOMA scheme over state-of-the-art approaches, i.e., the conventional FD [7], FD-NOMA with random UA and HD-NOMA.

Notation: $\mathbf{X}^T$, $\mathbf{X}^H$ and $\mathrm{tr}(\mathbf{X})$ are the transpose, Hermitian transpose and trace of a matrix $\mathbf{X}$, respectively. $\Re\{\cdot\}$ returns the real part of the argument. $\mathbf{x} \sim \mathcal{CN}(\boldsymbol{\eta}, \boldsymbol{Z})$ means that $\mathbf{x}$ is a random vector following a circularly symmetric complex Gaussian distribution with mean $\boldsymbol{\eta}$ and covariance matrix $\boldsymbol{Z}$.

II. SYSTEM MODEL AND PROBLEM FORMULATION

Consider a small cell in which the BS is equipped with $N > 1$ antennas. To facilitate the NOMA operation, the cell is virtually partitioned into Z annular regions (or zones). As illustrated in Fig. 1, we number the zones/regions of $\mathcal{Z} \triangleq \{1, 2, \ldots, Z\}$ in ascending order w.r.t. their distance from the BS. Without loss of generality, we assume that each zone contains K DL users[1] leading to $M = ZK$ DL users in total.

The BS is assumed to be equipped with the circulator-

---

[1]Note that the following analysis is also applicable when zones have different numbers of DL users.
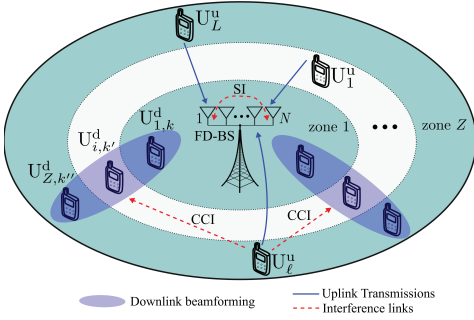
Fig. 1. A small cell FD-NOMA MU-MISO system. FD-BS serves $M = ZK$ DL users, with K DL users in each of the Z zones, and L UL users which are assumed to be uniformly deployed in the cell.

based FD radio prototypes [13] to simultaneously serve M and L single-antenna DL and UL users in the same frequency band, respectively. We denote the k-th DL user in zone i by $\mathtt{U}_{ik}^{\mathrm{d}}$, $\forall i \in \mathcal{Z}, k \in \mathcal{K} \triangleq \{1, 2, \ldots, K\}$, while the ℓ-th UL user at an arbitrary location is represented by $\mathtt{U}_\ell^{\mathrm{u}}$, $\forall \ell \in \mathcal{L} \triangleq \{1, 2, \ldots, L\}$. The channel vectors from the BS to $\mathtt{U}_{ik}^{\mathrm{d}}$ and from $\mathtt{U}_\ell^{\mathrm{u}}$ to the BS are denoted by $\mathbf{h}_{ik}^{\mathrm{d}} \in \mathbb{C}^{N \times 1}$ and $\mathbf{h}_\ell^{\mathrm{u}} \in \mathbb{C}^{N \times 1}$, respectively. To capture the imperfect SI suppression (SIS) at the BS, let $\mathbf{G}_{\mathrm{SI}} \in \mathbb{C}^{N \times N}$ and $\rho \in [0, 1)$ be the SI channel matrix and the residual SiS level, respectively. Further, let $g_{\ell, ik}$ denote the CCI channel from $\mathtt{U}_\ell^{\mathrm{u}}$ to $\mathtt{U}_{ik}^{\mathrm{d}}$.

A. Downlink Transmission

Before proceeding further, we first lay a foundation on the third-order tensor to generalize the DL user clustering, through the following definitions.

Definition 1: A cluster of DL users is a group consisting of Z DL users, in which no two DL users come from the same zone. The NOMA beamforming is thus applied to K different clusters. The third-order tensor $\mathbf{T} \triangleq [T_{kji}]_{k, j \in \mathcal{K}, i \in \mathcal{Z}}$ is used for UAs, where $T_{kji} \in \{0, 1\}$. If $T_{kji} = 1$, the j-th DL user in zone i is admitted to the k-th cluster, and vice versa.

Definition 2: It is clear that there are $K!$ possible permutations of clusters, and thus, the considered problem can be simplified by utilizing DL user indices in the first zone to index the clusters. In other words, the k-th DL user in the first zone is always admitted to the k-th cluster. $\mathbf{T}$ is formed by Z matrices w.r.t. the index i as $\mathbf{T} = \{\mathbf{C}_i\}_{i \in \mathcal{Z}}$, with $\mathbf{C}_i \triangleq [T_{kji}]_{k, j \in \mathcal{K}} \in \{0, 1\}^{K \times K}$ representing the i-th zone, and thus the first matrix of $\mathbf{T}$ is assigned to the identity matrix, i.e., $\mathbf{C}_1 \triangleq [T_{kj1}] = \mathbf{I}_K$. According to **Definition 1**, $\mathbf{C}_i$, $i \in \mathcal{Z} \backslash \{1\}$ is considered as the association variables of DL users.

From the two definitions above, we now establish the UA between two arbitrary zones as follows.

Theorem 1: Let $\mathbf{T}^{iz} \in \{0, 1\}^{K \times K}$, $\forall i, z \in \mathcal{Z}$ be an UA matrix between zones i and z. If the entry T_{kj}^{iz}, $\forall k, j \in \mathcal{K}$ is set to 1, the k-th DL user in zone i and the j-th DL user in zone z are grouped into the same cluster, and vice versa. Based on the structure of $\mathbf{T}$, the matrix $\mathbf{T}^{iz}$ is simply calculated as

$$\mathbf{T}^{iz} = \mathbf{C}_i^T \mathbf{C}_z. \tag{1}$$

Proof: Please see Appendix A. ∎

In the DL channel, BS employs a linear beamforming vector $\mathbf{w}_{ik} \in \mathbb{C}^{N \times 1}$ to precode the data symbol x_{ik}^{d}, with $\mathbb{E}\big[|x_{ik}^{\mathrm{d}}|^2\big] = 1$, intended to $\mathtt{U}_{ik}^{\mathrm{d}}$. The received signal at $\mathtt{U}_{ik}^{\mathrm{d}}$ can be expressed as

$$y_{ik}^{\mathrm{d}} = \sum_{i' \in \mathcal{Z}} \sum_{k' \in \mathcal{K}} (\mathbf{h}_{ik}^{\mathrm{d}})^H \mathbf{w}_{i'k'} x_{i'k'}^{\mathrm{d}} + \underbrace{\sum_{\ell \in \mathcal{L}} p_\ell g_{\ell, ik} x_\ell^{\mathrm{u}}}_{\text{CCI}} + n_{ik}, \tag{2}$$

where p_ℓ and x_ℓ^{u}, with $\mathbb{E}\big[|x_\ell^{\mathrm{u}}|^2\big] = 1$, are the transmit power coefficient and data symbol of $\mathtt{U}_\ell^{\mathrm{u}}$, respectively; and $n_{ik} \sim \mathcal{CN}(0, \sigma_{ik}^2)$ is the additive white Gaussian noise (AWGN) at $\mathtt{U}_{ik}^{\mathrm{d}}$. The messages intended to the DL user in cluster k are sequentially decoded as follows. $\mathtt{U}_{ik}^{\mathrm{d}}$ first decodes the messages of $\mathtt{U}_{i'j}^{\mathrm{d}}$ with $i' \in \mathcal{Z}_i^+ \triangleq \{i+1, \ldots, Z\}$ for $T_{kj}^{ii'} = 1$, and then removes them by using the SIC technique before decoding its own message. The received signal-to-interference-plus-noise ratio (SINR) at $\mathtt{U}_{ik}^{\mathrm{d}}$ can be generally expressed as

$$\gamma_{ik}^{\mathrm{d}}(\mathbf{w}, \mathbf{p}, \mathbf{T}) = \min_{z \in \mathcal{Z}_i^- \cup \{i\}} \max_{j \in \mathcal{K}} \left\{ \frac{T_{jk}^{zi} |(\mathbf{h}_{zj}^{\mathrm{d}})^H \mathbf{w}_{ik}|^2}{\Theta_{jk}^{zi}(\mathbf{w}, \mathbf{p}, \mathbf{T})} \right\}, \tag{3}$$

where $\mathcal{Z}_i^- \triangleq \{1, \ldots, i-1\}$, $\mathbf{p} = [p_\ell]_{\ell \in \mathcal{L}}$, $\mathbf{w} = [\mathbf{w}_i^H]_{i \in \mathcal{Z}}^H$ with $\mathbf{w}_i \triangleq [\mathbf{w}_{ik}]_{k \in \mathcal{K}}$, and the interference-plus-noise (IN) for decoding the $\mathtt{U}_{ik}^{\mathrm{d}}$'s message at $\mathtt{U}_{zj}^{\mathrm{d}}$, denoted by $\Theta_{jk}^{z;i}(\mathbf{w}, \mathbf{p})$, is given as

$$\Theta_{jk}^{zi}(\mathbf{w}, \mathbf{p}, \mathbf{T}) = \sum_{i' \in \mathcal{Z}} \sum_{k' \in \mathcal{K}} |(\mathbf{h}_{zj}^{\mathrm{d}})^H \mathbf{w}_{i'k'}|^2 + \sum_{\ell \in \mathcal{L}} p_\ell^2 |g_{\ell, zj}|^2$$
$$- \sum_{i' \in \mathcal{Z}_i^+ \cup \{i\}} \sum_{k' \in \mathcal{K}} T_{jk'}^{zi'} |(\mathbf{h}_{zj}^{\mathrm{d}})^H \mathbf{w}_{i'k'}|^2 + \sigma_{zj}^2. \tag{4}$$

B. Uplink Transmission

The received signal vector at the FD-BS in the UL transmission can be expressed as

$$\mathbf{y}^{\mathrm{u}} = \sum_{\ell \in \mathcal{L}} p_\ell \mathbf{h}_\ell^{\mathrm{u}} x_\ell^{\mathrm{u}} + \underbrace{\rho \sum_{i \in \mathcal{Z}} \sum_{k \in \mathcal{K}} \mathbf{G}_{\mathrm{SI}}^H \mathbf{w}_{ik} x_{ik}^{\mathrm{d}}}_{\text{SI}} + \mathbf{n}, \tag{5}$$

where $\mathbf{n} \sim \mathcal{CN}(0, \sigma_{\mathrm{U}}^2 \mathbf{I})$ is the AWGN. To decode the UL messages, we adopt the minimum mean-square error and SIC (MMSE-SIC) decoder at the FD-BS [14]. To jointly optimize the UL users' decoding order, we introduce binary variables $\beta_{\ell m} \in \{0, 1\}, \forall \ell, m \in \mathcal{L}$. Specifically, the message of the ℓ-th UL user is successfully decoded prior to that of the m-th UL user if $\beta_{\ell m} = 1$ in sync with $\beta_{m\ell} = 0$, and they are in reverse order if $\beta_{\ell m} = 0$. Accordingly, the received SINR of $\mathtt{U}_\ell^{\mathrm{u}}$ at the FD-BS can be expressed as

$$\gamma_\ell^{\mathrm{u}}(\mathbf{w}, \mathbf{p}, \boldsymbol{\beta}) = p_\ell^2 (\mathbf{h}_\ell^{\mathrm{u}})^H (\boldsymbol{\Psi}_\ell(\mathbf{w}, \mathbf{p}, \boldsymbol{\beta}))^{-1} \mathbf{h}_\ell^{\mathrm{u}}, \tag{6}$$

where

$$\boldsymbol{\Psi}_\ell(\mathbf{w}, \mathbf{p}, \boldsymbol{\beta}) \triangleq \sum_{m \in \mathcal{L}} \beta_{\ell m} p_m^2 \mathbf{h}_m^{\mathrm{u}} (\mathbf{h}_m^{\mathrm{u}})^H$$
$$+ \rho^2 \sum_{i \in \mathcal{Z}} \sum_{k \in \mathcal{K}} \mathbf{G}_{\mathrm{SI}}^H \mathbf{w}_{ik} \mathbf{w}_{ik}^H \mathbf{G}_{\mathrm{SI}} + \sigma_{\mathrm{U}}^2 \mathbf{I}.$$

C. Problem Formulation

With the above discussion, the achievable rate in nats/s/Hz of $\mathtt{U}_{ik}^{\mathrm{d}}$ and $\mathtt{U}_\ell^{\mathrm{u}}$ are respectively given as $R_{ik}^{\mathrm{d}}(\mathbf{w}, \mathbf{p}, \mathbf{T}) = \ln(1 + \gamma_{ik}^{\mathrm{d}}(\mathbf{w}, \mathbf{p}, \mathbf{T}))$ and $R_\ell^{\mathrm{u}}(\mathbf{w}, \mathbf{p}, \boldsymbol{\beta}) = \ln(1 + \gamma_\ell^{\mathrm{u}}(\mathbf{w}, \mathbf{p}, \boldsymbol{\beta}))$. We

can now state the SR maximization problem under the quality-of-service (QoS) and power constraints (SRM problem for short) as

$$\max_{\mathbf{w},\mathbf{p},\mathbf{T},\boldsymbol{\beta}} R_\Sigma \triangleq \sum_{i\in\mathcal{Z}}\sum_{k\in\mathcal{K}} R_{ik}^{\mathrm{d}}(\mathbf{w},\mathbf{p},\mathbf{T}) + \sum_{\ell\in\mathcal{L}} R_\ell^{\mathrm{u}}(\mathbf{w},\mathbf{p},\boldsymbol{\beta}) \quad (7a)$$

$$\text{s.t.} \quad \|\mathbf{w}\|^2 \leq P_{\mathrm{bs}}^{\max}, \quad (7b)$$

$$p_\ell^2 \leq P_\ell^{\max},\ p_\ell \geq 0,\ \forall \ell \in \mathcal{L}, \quad (7c)$$

$$R_{ik}^{\mathrm{d}}(\mathbf{w},\mathbf{p},\mathbf{T}) \geq \bar{R}_{ik}^{\mathrm{d}},\ \forall i \in \mathcal{Z},\ k \in \mathcal{K}, \quad (7d)$$

$$R_\ell^{\mathrm{u}}(\mathbf{w},\mathbf{p},\boldsymbol{\beta}) \geq \bar{R}_\ell^{\mathrm{u}},\ \forall \ell \in \mathcal{L}, \quad (7e)$$

$$T_{kj}^{iz} \in \{0,1\},\ \forall i,z \in \mathcal{Z},\ \forall k,j \in \mathcal{K}, \quad (7f)$$

$$\sum_{k\in\mathcal{K}} T_{kj}^{iz} = 1,\ \sum_{j\in\mathcal{K}} T_{kj}^{iz} = 1, \forall i,z \in \mathcal{Z},\ \forall k,j \in \mathcal{K}, \quad (7g)$$

$$\beta_{\ell m} \in \{0,1\},\ \forall \ell, m \in \mathcal{L}, \quad (7h)$$

$$\beta_{\ell\ell} = 0,\ \forall \ell \in \mathcal{L}, \quad (7i)$$

$$\beta_{\ell m} + \beta_{m\ell} = 1,\ \ell \neq m,\ \forall \ell, m \in \mathcal{L}, \quad (7j)$$

$$\Big|\sum_{m\in\mathcal{L}} \beta_{\ell m} - \sum_{m\in\mathcal{L}} \beta_{\ell' m}\Big| \geq 1,\ \ell \neq \ell',\ \forall \ell, \ell' \in \mathcal{L}, \quad (7k)$$

where $P_{\mathrm{bs}}^{\max}$ and $P_\ell^{\max}$ in (7b) and (7c) are the transmit power budgets at the BS and $\mathtt{U}_\ell^{\mathrm{u}}$, respectively. In (7d) and (7e), we impose the minimum QoS requirements $\bar{R}_{ik}^{\mathrm{d}} \geq 0$ and $\bar{R}_\ell^{\mathrm{u}} \geq 0$ in order to maintain some degree of fairness among users. Constraints (7f) and (7g) establish the criteria for DL user clustering, in which $\mathbf{T}^{iz}$ satisfies the property of tensor $\mathbf{T}$ given in **Theorem 1**, while constraints (7h)-(7k) determine the decoding orders of UL users. Obviously, problem (7) belongs to a class of mixed-integer non-convex problem.

Remark *1:* The merits of **Theorem 1** to problem (7) are as follows. Firstly, since $\mathbf{C}_1$ is fixed to identity matrix, the association problem avoids searching all permutations of clusters while still achieving a close-to-optimal solution. The second advantage is to reduce the number of association variables by utilizing the relationship among $\mathbf{T}^{iz}$, $i,z \in \mathcal{Z}$.

Case study with $Z = 2$: As pointed out in [15], a larger cluster size with the distinct channel conditions among DL users is more desirable in the NOMA system. In this paper, we focus on a small-cell setup due to current practical limitations of FD radios [6]–[9]. As such, we will study user pairing (each pair including one near DL user $\mathtt{U}_{1k}^{\mathrm{d}}$ in the inner zone and one far DL user $\mathtt{U}_{2j}^{\mathrm{d}}$ in the outer zone) for DL transmission to reduce the system load, which has been widely adopted in the literature [6], [16]. In this case, $\mathbf{T}$ includes two UA matrices as $\mathbf{C}_1 = \mathbf{I}_K$ and $\mathbf{C}_2 \in \{0,1\}^{K\times K}$. For convenience, let $\boldsymbol{\alpha} = \mathbf{T}^{12} = \mathbf{C}_2$ be a unique matrix of UA variables in $\mathbf{T}$, and then the entries of $\boldsymbol{\alpha}$ are $\alpha_{kj} \in \{0,1\}$, indicating whether $\mathtt{U}_{1k}^{\mathrm{d}}$ in zone 1 is paired with $\mathtt{U}_{2j}^{\mathrm{d}}$ in zone 2. From (3), the SINRs at $\mathtt{U}_{1k}^{\mathrm{d}}$ and $\mathtt{U}_{2j}^{\mathrm{d}}$ are respectively simplified as

$$\gamma_{1k}^{\mathrm{d}}(\mathbf{w},\mathbf{p},\boldsymbol{\alpha}) = \frac{|(\mathbf{h}_{1k}^{\mathrm{d}})^H \mathbf{w}_{1k}|^2}{\phi_k(\mathbf{w},\mathbf{p},\boldsymbol{\alpha})}, \quad (8a)$$

$$\gamma_{2j}^{\mathrm{d}}(\mathbf{w},\mathbf{p},\boldsymbol{\alpha}) = \min\left\{ \max_{k\in\mathcal{K}}\left\{ \frac{\alpha_{kj}|(\mathbf{h}_{1k}^{\mathrm{d}})^H \mathbf{w}_{2j}|^2}{\psi_j^k(\mathbf{w},\mathbf{p})} \right\}, \frac{|(\mathbf{h}_{2j}^{\mathrm{d}})^H \mathbf{w}_{2j}|^2}{\varphi_j(\mathbf{w},\mathbf{p})} \right\}, \quad (8b)$$

where the IN $\phi_k(\mathbf{w},\mathbf{p},\boldsymbol{\alpha})$ experienced by $\mathtt{U}_{1k}^{\mathrm{d}}$ is $\phi_k(\mathbf{w},\mathbf{p},\boldsymbol{\alpha}) = \sum_{k'\in\mathcal{K}\setminus k}|(\mathbf{h}_{1k}^{\mathrm{d}})^H \mathbf{w}_{1k'}|^2 + \sum_{\ell\in\mathcal{L}} p_\ell^2 |g_{\ell,1k}|^2 + \sum_{j'\in\mathcal{K}}(1-\alpha_{kj'})|(\mathbf{h}_{1k}^{\mathrm{d}})^H \mathbf{w}_{2j'}|^2 + \sigma_{1k}^2$, while the INs involved in the SINRs for decoding the $\mathtt{U}_{2j}^{\mathrm{d}}$'s message at $\mathtt{U}_{1k}^{\mathrm{d}}$ and

itself are given as $\psi_j^k(\mathbf{w},\mathbf{p}) \triangleq \sum_{k'\in\mathcal{K}}|(\mathbf{h}_{1k}^{\mathrm{d}})^H \mathbf{w}_{1k'}|^2 + \sum_{j'\in\mathcal{K}\setminus j}|(\mathbf{h}_{1k}^{\mathrm{d}})^H \mathbf{w}_{2j'}|^2 + \sum_{\ell\in\mathcal{L}} p_\ell^2 |g_{\ell,1k}|^2 + \sigma_{1k}^2$, and $\varphi_j(\mathbf{w},\mathbf{p}) \triangleq \sum_{k'\in\mathcal{K}}|(\mathbf{h}_{2j}^{\mathrm{d}})^H \mathbf{w}_{1k'}|^2 + \sum_{j'\in\mathcal{K}\setminus j}|(\mathbf{h}_{2j}^{\mathrm{d}})^H \mathbf{w}_{2j'}|^2 + \sum_{\ell\in\mathcal{L}} p_\ell^2 |g_{\ell,2j}|^2 + \sigma_{2j}^2$, respectively. We remark that the first term in (8b) is the SINR for decoding the $\mathtt{U}_{2j}^{\mathrm{d}}$'s message at $\mathtt{U}_{1k}^{\mathrm{d}}$, which is imposed on $\gamma_{2j}^{\mathrm{d}}(\mathbf{w},\mathbf{p},\boldsymbol{\alpha})$ to ensure that $\mathtt{U}_{1k}^{\mathrm{d}}$ can successfully decode the $\mathtt{U}_{2j}^{\mathrm{d}}$'s message by SIC [15]. Toward this end, we consider the following modification of (7)

$$\max_{\mathbf{w},\mathbf{p},\boldsymbol{\alpha},\boldsymbol{\beta}} R_\Sigma \triangleq \sum_{i\in\mathcal{Z}}\sum_{k\in\mathcal{K}} R_{ik}^{\mathrm{d}}(\mathbf{w},\mathbf{p},\boldsymbol{\alpha}) + \sum_{\ell\in\mathcal{L}} R_\ell^{\mathrm{u}}(\mathbf{w},\mathbf{p},\boldsymbol{\beta}) \quad (9a)$$

$$\text{s.t.} \quad (7b),(7c),(7e),(7h)-(7k), \quad (9b)$$

$$R_{ik}^{\mathrm{d}}(\mathbf{w},\mathbf{p},\boldsymbol{\alpha}) \geq \bar{R}_{ik}^{\mathrm{d}},\ \forall i \in \mathcal{Z}, k \in \mathcal{K}, \quad (9c)$$

$$\alpha_{kj} \in \{0,1\},\ \forall k,j \in \mathcal{K}, \quad (9d)$$

$$\sum_{k\in\mathcal{K}} \alpha_{kj} = 1,\ \sum_{j\in\mathcal{K}} \alpha_{kj} = 1, \forall k,j \in \mathcal{K}. \quad (9e)$$

III. PROPOSED SOLUTION FOR (9)

To begin with, we transform problem (9) to the continuous relaxation (CR) form using the PFs as follows:

$$\max_{\mathbf{w},\mathbf{p},\boldsymbol{\alpha},\boldsymbol{\beta}} \sum_{i\in\mathcal{Z}}\sum_{k\in\mathcal{K}} R_{ik}^{\mathrm{d}}(\mathbf{w},\mathbf{p},\boldsymbol{\alpha}) + \sum_{\ell\in\mathcal{L}} R_\ell^{\mathrm{u}}(\mathbf{w},\mathbf{p},\boldsymbol{\beta}) + F_p \quad (10a)$$

$$\text{s.t.} \quad (7b),(7c),(7e),(7i)-(7k),(9c),(9e), \quad (10b)$$

$$0 \leq \alpha_{kj} \leq 1,\ \forall k,j \in \mathcal{K}, \quad (10c)$$

$$0 \leq \beta_{\ell m} \leq 1,\ \forall \ell, m \in \mathcal{L}, \quad (10d)$$

where $\boldsymbol{\alpha}$ and $\boldsymbol{\beta}$ are relaxed to be continuous as in (10c) and (10d), respectively. We define $F_p \triangleq \sum_{k\in\mathcal{K}}\sum_{j\in\mathcal{K}} \varrho_{kj}^{\mathrm{d}} f_p(\alpha_{kj}) + \sum_{\ell\in\mathcal{L}}\sum_{m\in\mathcal{L}} \varrho_{\ell m}^{\mathrm{u}} f_p(\beta_{\ell m})$, where $f_p(x) \triangleq x^2 - x$, and $\varrho_{kj}^{\mathrm{d}} > 0$ and $\varrho_{\ell m}^{\mathrm{u}} > 0$ are the penalty parameters. It is obvious that the difficulty in solving problem (10) is due to the non-concave objective function (10a) and non-convex constraints in (7e), (7k), and (9c).

Concavity of the objective (10a)*:* Let us start by handling the non-concavity of $R_{ik}^{\mathrm{d}}(\mathbf{w},\mathbf{p},\boldsymbol{\alpha})$. For $\mathtt{U}_{1k}^{\mathrm{d}}$ (DL users in zone 1), we introduce new variales $\omega_{1k}, \forall k \in \mathcal{K}$ to explicitly expose the non-convex parts of $R_{1k}^{\mathrm{d}}(\mathbf{w},\mathbf{p},\boldsymbol{\alpha})$ as

$$R_{1k}^{\mathrm{d}}(\mathbf{w},\mathbf{p},\boldsymbol{\alpha}) \geq \ln\big(1 + \frac{1}{\omega_{1k}}\big), \quad (11a)$$

$$\frac{|(\mathbf{h}_{1k}^{\mathrm{d}})^H \mathbf{w}_{1k}|^2}{\phi_k(\mathbf{w},\mathbf{p},\boldsymbol{\alpha})} \geq \frac{1}{\omega_{1k}}, \quad (11b)$$

which does not affect the optimality. From (11a) and as an effort to reduce the complexity, the concave minorant of $R_{1k}^{\mathrm{d}}(\mathbf{w},\mathbf{p},\boldsymbol{\alpha})$ at the $(\kappa+1)$-th iteration is derived as

$$R_{1k}^{\mathrm{d}}(\mathbf{w},\mathbf{p},\boldsymbol{\alpha}) \geq \mathtt{A}(\omega_{1k}^{(\kappa)}) + \mathtt{B}(\omega_{1k}^{(\kappa)})\omega_{1k} := \ddot{R}_{1k}^{\mathrm{d},(\kappa)}, \quad (12)$$

due to the convexity of $\ln\big(1 + \frac{1}{\omega_{1k}}\big)$, where $\mathtt{A}(\omega_{1k}^{(\kappa)}) \triangleq \ln\big(1 + \frac{1}{\omega_{1k}^{(\kappa)}}\big) + \frac{1}{(\omega_{1k}^{(\kappa)}+1)}$ and $\mathtt{B}(\omega_{1k}^{(\kappa)}) \triangleq -\frac{1}{\omega_{1k}^{(\kappa)}(\omega_{1k}^{(\kappa)}+1)}$ [15, Eq. (82)]. Obviously, we obtain $R_{1k}^{\mathrm{d}}(\mathbf{w},\mathbf{p},\boldsymbol{\alpha}) = \ddot{R}_{1k}^{\mathrm{d},(\kappa)}$ as $\kappa \to \infty$. By applying the ICA method, we iteratively replace the non-convex constraint (11b) by

$$\phi_k(\mathbf{w},\mathbf{p},\boldsymbol{\alpha}) \leq \omega_{1k}\tilde{\gamma}_{1k}^{(\kappa)}(\mathbf{w}), \quad (13)$$

over the trust region (i.e., the feasible domain):

$$\tilde{\gamma}_{1k}^{(\kappa)}(\mathbf{w}) \triangleq 2\Re\{(\mathbf{h}_{1k}^{\mathrm{d}})^H \mathbf{w}_{1k}^{(\kappa)}\}\Re\{(\mathbf{h}_{1k}^{\mathrm{d}})^H \mathbf{w}_{1k}\}$$
$$- \big(\Re\{(\mathbf{h}_{1k}^{\mathrm{d}})^H \mathbf{w}_{1k}^{(\kappa)}\}\big)^2 > 0,\ \forall k \in \mathcal{K}, \quad (14)$$

where $\tilde{\gamma}_{1k}^{(\kappa)}(\mathbf{w})$ is the first order approximation of

$|(\mathbf{h}_{1k}^{\mathrm{d}})^H \mathbf{w}_{1k}|^2$ around the point $\mathbf{w}_{1k}^{(\kappa)}$ found at iteration κ. To address the non-convexity of (13), we introduce the following lemma.

Lemma 1: Consider a function $h(x,y) \triangleq xy^2$, $x > 0$. The convex majorant of $h(x,y)$ is expressed as

$$h(x,y) \leq \frac{z^{(\kappa)}}{2x^{(\kappa)}}x^2 + \frac{x^{(\kappa)}}{2z^{(\kappa)}}z^2 \triangleq \tilde{h}^{(\kappa)}(x,z), \quad (15)$$

by imposing a second-order cone (SOC) constraint: $y^2 \leq z$, where $z > 0$ is a new variable.

Proof: The proof is omitted due to the space limitation. ■

From Lemma 1, the convex upper bound of $\phi_k(\mathbf{w},\mathbf{p},\boldsymbol{\alpha})$ is

$$\phi_k(\mathbf{w},\mathbf{p},\boldsymbol{\alpha}) \leq \tilde{\phi}_k^{(\kappa)}(\mathbf{w},\mathbf{p},\boldsymbol{\lambda},\boldsymbol{\mu}), \quad (16)$$

where $\tilde{\phi}_k^{(\kappa)}(\mathbf{w},\mathbf{p},\boldsymbol{\lambda},\boldsymbol{\mu}) \triangleq \sum_{k' \in \mathcal{K}\setminus k} |(\mathbf{h}_{1k}^{\mathrm{d}})^H \mathbf{w}_{1k'}|^2 + \sum_{\ell \in \mathcal{L}} p_\ell^2 |g_{\ell,1k}|^2 + \sum_{j' \in \mathcal{K}} \tilde{h}^{(\kappa)}(\lambda_{kj'},\mu_{kj'}) + \sigma_{1k}^2$, $\boldsymbol{\lambda} \triangleq [\lambda_{kj}]_{k,j \in \mathcal{K}}$ and $\boldsymbol{\mu} \triangleq [\mu_{kj}]_{k,j \in \mathcal{K}}$ are alternative variables, in which λ_{kj} and μ_{kj} satisfy the following convex constraints:

$$\lambda_{kj} = 1 - \alpha_{kj}, \forall k,j \in \mathcal{K}, \quad (17a)$$

$$|(\mathbf{h}_{1k}^{\mathrm{d}})^H \mathbf{w}_{2j}|^2 \leq \mu_{kj}, \quad \forall k,j \in \mathcal{K}. \quad (17b)$$

In this regard, we iteratively replace (13) by the convex constraint:

$$\tilde{\phi}_k^{(\kappa)}(\mathbf{w},\mathbf{p},\boldsymbol{\lambda},\boldsymbol{\mu}) \leq \omega_{1k}\tilde{\gamma}_{1k}^{(\kappa)}(\mathbf{w}), \forall k \in \mathcal{K}, \quad (18)$$

which is the SOC representative. To address $R_{2j}^{\mathrm{d}}(\mathbf{w},\mathbf{p},\boldsymbol{\alpha})$, we can equivalently express the SINR γ_{2j}^{d} of $\mathsf{U}_{2j}^{\mathrm{d}}$ (DL users in zone 2) as

$$\gamma_{2j}^{\mathrm{d}}(\mathbf{w},\mathbf{p},\boldsymbol{\alpha}) = \min\left\{\min_{k\in\mathcal{K}}\left\{\frac{|(\mathbf{h}_{1k}^{\mathrm{d}})^H\mathbf{w}_{2j}|^2}{\alpha_{kj}\psi_j^k(\mathbf{w},\mathbf{p})}\right\}, \frac{|(\mathbf{h}_{2j}^{\mathrm{d}})^H\mathbf{w}_{2j}|^2}{\varphi_j(\mathbf{w},\mathbf{p})}\right\}. (19)$$

We replace α_{kj} by $\alpha_{kj} + \varepsilon$ to avoid the numerical problem design when $\alpha_{kj} = 0$, where ε is a given small number. In the same manner to (12), the non-smoothness and non-concavity of $R_{2j}^{\mathrm{d}}(\mathbf{w},\mathbf{p},\boldsymbol{\alpha})$ are tackled as

$$R_{2j}^{\mathrm{d}}(\mathbf{w},\mathbf{p},\boldsymbol{\alpha}) \geq \mathtt{A}(\omega_{2j}^{(\kappa)}) + \mathtt{B}(\omega_{2j}^{(\kappa)})\omega_{2j} := \ddot{R}_{2j}^{\mathrm{d},(\kappa)}, \quad (20)$$

by imposing the following constraints

$$\frac{|(\mathbf{h}_{1k}^{\mathrm{d}})^H\mathbf{w}_{2j}|^2}{(\alpha_{kj}+\varepsilon)\psi_j^k(\mathbf{w},\mathbf{p})} \geq \frac{1}{\omega_{2j}}, \text{ and } \frac{|(\mathbf{h}_{2j}^{\mathrm{d}})^H\mathbf{w}_{2j}|^2}{\varphi_j(\mathbf{w},\mathbf{p})} \geq \frac{1}{\omega_{2j}}. (21)$$

As in (11b), the non-convex constraints (21) are innerly convexified by

$$\psi_j^k(\mathbf{w},\mathbf{p}) \leq \omega_{2j}\ddot{\gamma}_{2,kj}^{(\kappa)}(\mathbf{w},\boldsymbol{\alpha}), \forall k,j \in \mathcal{K}, \quad (22a)$$

$$\varphi_j(\mathbf{w},\mathbf{p}) \leq \omega_{2j}\tilde{\gamma}_{2j}^{(\kappa)}(\mathbf{w}), \forall j \in \mathcal{K}, \quad (22b)$$

over the trust regions:

$$\ddot{\gamma}_{2,kj}^{(\kappa)}(\mathbf{w},\boldsymbol{\alpha}) \triangleq \frac{2\Re\{((\mathbf{h}_{1k}^{\mathrm{d}})^H\mathbf{w}_{2j}^{(\kappa)})^*((\mathbf{h}_{1k}^{\mathrm{d}})^H\mathbf{w}_{2j})\}}{\alpha_{kj}^{(\kappa)}+\varepsilon}$$
$$- \frac{|(\mathbf{h}_{1k}^{\mathrm{d}})^H\mathbf{w}_{2j}^{(\kappa)}|^2}{(\alpha_{kj}^{(\kappa)}+\varepsilon)^2}(\alpha_{kj}+\varepsilon) > 0, \forall k,j \in \mathcal{K}, (23a)$$

$$\tilde{\gamma}_{2j}^{(\kappa)}(\mathbf{w}) \triangleq 2\Re\{(\mathbf{h}_{2j}^{\mathrm{d}})^H\mathbf{w}_{2j}^{(\kappa)}\}\Re\{(\mathbf{h}_{2j}^{\mathrm{d}})^H\mathbf{w}_{2j}\}$$
$$- (\Re\{(\mathbf{h}_{2j}^{\mathrm{d}})^H\mathbf{w}_{2j}^{(\kappa)}\})^2 > 0, \forall j \in \mathcal{K}. \quad (23b)$$

Next, at the feasible point $(\mathbf{w}^{(\kappa)},\mathbf{p}^{(\kappa)},\boldsymbol{\beta}^{(\kappa)})$, the UL rate function $R_\ell^{\mathrm{u}}(\mathbf{w},\mathbf{p},\boldsymbol{\beta})$ is globally lower bounded by

$$R_\ell^{\mathrm{u}}(\mathbf{w},\mathbf{p},\boldsymbol{\beta}) \geq \tilde{\mathtt{A}}_\ell^{(\kappa)}(p_\ell) - \Phi_\ell^{(\kappa)}(\mathbf{w},\mathbf{p},\boldsymbol{\beta}), \quad (24)$$

where $\tilde{\mathtt{A}}_\ell^{(\kappa)}(p_\ell) \triangleq \ln(1 + \gamma_\ell^{\mathrm{u}}(\mathbf{w}^{(\kappa)},\mathbf{p}^{(\kappa)},\boldsymbol{\beta}^{(\kappa)})) - \gamma_\ell^{\mathrm{u}}(\mathbf{w}^{(\kappa)},\mathbf{p}^{(\kappa)},\boldsymbol{\beta}^{(\kappa)})(\frac{2p_\ell}{p_\ell^{(\kappa)}}-1)$, $\Phi_\ell^{(\kappa)}(\mathbf{w},\mathbf{p},\boldsymbol{\beta}) \triangleq \sigma_{\mathsf{U}}^2\mathrm{tr}(\Xi_\ell^{(\kappa)}) +$

$p_\ell^2(\mathbf{h}_\ell^{\mathrm{u}})^H\Xi_\ell^{(\kappa)}\mathbf{h}_\ell^{\mathrm{u}} + \sum_{m\in\mathcal{L}\setminus\ell}\beta_{\ell m}p_m^2(\mathbf{h}_m^{\mathrm{u}})^H\Xi_\ell^{(\kappa)}\mathbf{h}_m^{\mathrm{u}} + \rho^2\sum_{k\in\mathcal{K}}(\mathbf{w}_k)^H\mathbf{G}_{\mathrm{SI}}\Xi_\ell^{(\kappa)}\mathbf{G}_{\mathrm{SI}}^H\mathbf{w}_k$, in which we have

$$\Xi_\ell^{(\kappa)} \triangleq (\Psi_\ell^{(\kappa)})^{-1} - ((p_\ell^{(\kappa)})^2\mathbf{h}_\ell^{\mathrm{u}}(\mathbf{h}_\ell^{\mathrm{u}})^H + \Psi_\ell^{(\kappa)})^{-1},$$

with $\Psi_\ell^{(\kappa)} \triangleq \sigma_{\mathsf{U}}^2\mathbf{I} + \sum_{m\in\mathcal{L}\setminus\ell}\beta_{\ell m}^{(\kappa)}(p_m^{(\kappa)})^2\mathbf{h}_m^{\mathrm{u}}(\mathbf{h}_m^{\mathrm{u}})^H + \rho^2\sum_{k\in\mathcal{K}}\mathbf{G}_{\mathrm{SI}}^H\mathbf{w}_k^{(\kappa)}(\mathbf{w}_k^{(\kappa)})^H\mathbf{G}_{\mathrm{SI}}$. To convexify the right-hand side of (24), we apply **Lemma 1** to the second term of $\Phi_\ell^{(\kappa)}(\mathbf{w},\mathbf{p},\boldsymbol{\beta})$. It is true that $\Phi_\ell^{(\kappa)}(\mathbf{w},\mathbf{p},\boldsymbol{\beta}) \leq \tilde{\Phi}_\ell^{(\kappa)}(\mathbf{w},\mathbf{p},\boldsymbol{\beta},\boldsymbol{\nu})$, where $\tilde{\Phi}_\ell^{(\kappa)}(\mathbf{w},\mathbf{p},\boldsymbol{\beta},\boldsymbol{\nu}) \triangleq p_\ell^2(\mathbf{h}_\ell^{\mathrm{u}})^H\Xi_\ell^{(\kappa)}\mathbf{h}_\ell^{\mathrm{u}} + \rho^2\sum_{k\in\mathcal{K}}(\mathbf{w}_k)^H\mathbf{G}_{\mathrm{SI}}\Xi_\ell^{(\kappa)}\mathbf{G}_{\mathrm{SI}}^H\mathbf{w}_k + \sum_{m\in\mathcal{L}\setminus\ell}\tilde{h}^{(\kappa)}(\beta_{\ell m},\nu_m)(\mathbf{h}_m^{\mathrm{u}})^H\Xi_m^{(\kappa)}\mathbf{h}_m^{\mathrm{u}} + \sigma_{\mathsf{U}}^2\mathrm{tr}(\Xi_\ell^{(\kappa)})$, with the additional SOC and linear constraints:

$$p_m^2 \leq \nu_m \leq P_m^{\max}, \quad \forall m \in \mathcal{L}, \quad (25)$$

where $\boldsymbol{\nu} \triangleq [\nu_m]_{m\in\mathcal{L}}$ are new variables. The concave quadratic minorant of $R_\ell^{\mathrm{u}}(\mathbf{w},\mathbf{p},\boldsymbol{\beta})$ at iteration $\kappa+1$ is given by

$$R_\ell^{\mathrm{u}}(\mathbf{w},\mathbf{p},\boldsymbol{\beta}) \geq \tilde{\mathtt{A}}_\ell^{(\kappa)}(p_\ell) - \tilde{\Phi}_\ell^{(\kappa)}(\mathbf{w},\mathbf{p},\boldsymbol{\beta},\boldsymbol{\nu}) := \ddot{R}_\ell^{\mathrm{u},(\kappa)}. (26)$$

Finally, we apply the ICA method to $f_p(x)$, given as $f_p(x) \geq (2x^{(\kappa)} - 1)x - (x^{(\kappa)})^2 := \tilde{f}_p^{(\kappa)}(x)$, where $x^{(\kappa)}$ is a feasible point at iteration κ. Clearly, the objective function and constraints (7e), (9c) are innerly convexified by replacing the non-concave functions $R_{ik}^{\mathrm{d}}(\mathbf{w},\mathbf{p},\boldsymbol{\alpha})$ and $R_\ell^{\mathrm{u}}(\mathbf{w},\mathbf{p},\boldsymbol{\beta})$ with the concave functions $\ddot{R}_{ik}^{\mathrm{d},(\kappa)}$ and $\ddot{R}_\ell^{\mathrm{u},(\kappa)}$, respectively, while $f_p(\alpha_{kj})$ and $f_p(\beta_{\ell m})$ in F_p are replaced by $\tilde{f}_p^{(\kappa)}(\alpha_{kj})$ and $\tilde{f}_p^{(\kappa)}(\beta_{\ell m})$, respectively.

Convexity of constraint (7k)*:* To handle the non-convexity of (7k), we first replace the absolute function with the maximum function as:

$$|s_{\ell\ell'}| = \max(s_{\ell\ell'}, -s_{\ell\ell'}) \geq 1, \ell \neq \ell', \forall \ell,\ell' \in \mathcal{L},$$

where $s_{\ell\ell'} \triangleq \sum_{m=1}^L \beta_{\ell m} - \sum_{m=1}^L \beta_{\ell' m}$. Then, a smooth approximation, which exploits the log-sum-exp form, is applied to the max function, i.e., $\max(s_{\ell\ell'}, -s_{\ell\ell'}) \geq f_{\mathrm{LSE}}(s_{\ell\ell'})$, where $f_{\mathrm{LSE}}(s_{\ell\ell'}) \triangleq \frac{1}{\Omega}\ln\left(\frac{\exp(\Omega s_{\ell\ell'}) + \exp(-\Omega s_{\ell\ell'})}{2}\right)$, with Ω being a predefined large number. By applying the ICA method to $f_{\mathrm{LSE}}(s_{\ell\ell'})$ around the point $s_{\ell\ell'}^{(\kappa)} \triangleq \sum_{m=1}^L \beta_{\ell m}^{(\kappa)} - \sum_{m=1}^L \beta_{\ell' m}^{(\kappa)}$, (7k) is replaced by the following linear constraint:

$$f_{\mathrm{LSE}}^{(\kappa)}(s_{\ell\ell'}) \geq 1, \ell \neq \ell', \forall \ell,\ell' \in \mathcal{L}, \quad (27)$$

where

$$f_{\mathrm{LSE}}^{(\kappa)}(s_{\ell\ell'}) \triangleq f_{\mathrm{LSE}}(s_{\ell\ell'}^{(\kappa)}) + \frac{\partial f_{\mathrm{LSE}}}{\partial s_{\ell\ell'}}\Big|_{s_{\ell\ell'}=s_{\ell\ell'}^{(\kappa)}}(s_{\ell\ell'} - s_{\ell\ell'}^{(\kappa)}).$$

From the discussions above, the successive convex program to solve (10) at iteration $\kappa+1$ is given as:

$$\max_{\mathbf{X}} \quad \mathring{R}_\Sigma^{(\kappa+1)} \triangleq \ddot{R}_\Sigma^{(\kappa)} + \tilde{F}_p^{(\kappa)} \quad (28a)$$

$$\text{s.t.} \quad (7b), (7i), (7j), (9e), (10c), (10d),$$

$$(14), (17), (18), (22), (23), (25), (27), \quad (28b)$$

$$\ddot{R}_{ik}^{\mathrm{d},(\kappa)} \geq \bar{R}_{ik}^{\mathrm{d}}, \forall i \in \mathcal{Z}, k \in \mathcal{K}, \quad (28c)$$

$$\ddot{R}_\ell^{\mathrm{u},(\kappa)} \geq \bar{R}_\ell^{\mathrm{u}}, \forall \ell \in \mathcal{L}, \quad (28d)$$

where $\ddot{R}_\Sigma^{(\kappa)} \triangleq \sum_{i\in\mathcal{Z}}\sum_{k\in\mathcal{K}}\ddot{R}_{ik}^{\mathrm{d},(\kappa)} + \sum_{\ell\in\mathcal{L}}\ddot{R}_\ell^{\mathrm{u},(\kappa)}$, $\tilde{F}_p^{(\kappa)} \triangleq \sum_{k\in\mathcal{K}}\sum_{j\in\mathcal{K}}\varrho_{kj}^{\mathrm{d}}\tilde{f}_p^{(\kappa)}(\alpha_{kj}) + \sum_{\ell\in\mathcal{L}}\sum_{m\in\mathcal{L}}\varrho_{\ell m}^{\mathrm{u}}\tilde{f}_p^{(\kappa)}(\beta_{\ell m})$, and $\mathbf{X} \triangleq \{\mathbf{w},\mathbf{p},\boldsymbol{\alpha},\boldsymbol{\beta},\boldsymbol{\omega},\boldsymbol{\lambda},\boldsymbol{\mu},\boldsymbol{\nu}\}$, with $\boldsymbol{\omega} \triangleq [\omega_{ik}]_{i\in\mathcal{Z},k\in\mathcal{K}}$. To summarize, **Algorithm 1** outlines the proposed algorithm to solve (10), referred to as ICA-CR-PF. Without loss of optimality, the constant penalty parameters can be uniformly selected through $\varrho \triangleq \max\{\varrho_{kj}^{\mathrm{d}}, \varrho_{\ell m}^{\mathrm{u}}\}_{k,j\in\mathcal{K}, \ell,m\in\mathcal{L}}$.

Algorithm 1 Proposed ICA-CR-PF for Problem (10)

1: **Initialization:** Set $R_\Sigma := -\infty$ and $(\mathbf{w}^*, \mathbf{p}^*, \boldsymbol{\alpha}^*, \boldsymbol{\beta}^*) := \mathbf{0}$.
2: Set $\kappa := 0$ and generate an initial feasible point $\mathbf{X}^{(0)}$.
3: **repeat**
4:      Set $\varrho_{kj}^{\mathrm{d}} = \varrho_{\ell m}^{\mathrm{u}} = \varrho, \ \forall k, j \in \mathcal{K}, \ \forall \ell, m \in \mathcal{L}$.
5:      Solve (28) to obtain $\mathbf{X}^\star$ and $\mathring{R}_\Sigma^{(\kappa+1)}$.
6:      Update $\mathbf{X}^{(\kappa+1)} := \mathbf{X}^\star$.
7:      Set $\kappa := \kappa + 1$.
8: **until** Convergence
9: Use $(\mathbf{w}^*, \mathbf{p}^*, \boldsymbol{\alpha}^*, \boldsymbol{\beta}^*)$ in $\mathbf{X}^{(\kappa)}$ to compute R_Σ as in (9a).
10: **Output:** R_Σ and the optimal solution $(\mathbf{w}^*, \mathbf{p}^*, \boldsymbol{\alpha}^*, \boldsymbol{\beta}^*)$.

Convergence Analysis: The optimal solutions achieved by the proposed algorithms at iteration κ are also feasible for the problem at iteration $\kappa + 1$, i.e., $\mathcal{F}^{(\kappa)} \subseteq \mathcal{F}^{(\kappa+1)}$, where $\mathcal{F}^{(\kappa)}$ denotes the convex feasible sets of (28) at iteration κ. Moreover, $\mathcal{F}^{(\kappa)}$ is closed and bounded due to the ICA method and the power constraints (7b) and (7c). The feasible sets $\mathcal{F}^{(\kappa)}$ are compact and non-empty, and thus it satisfies the connectedness condition for Karush-Kuhn-Tucker (KKT) invexity as $\kappa \to \infty$.

Complexity Analysis: We first observe that the convex programs given in (28) involve only the SOC and linear constraints, thus leading to low computational complexity. In particular, it takes a polynomial time complexity of $\mathcal{O}(c^{2.5}v^2 + c^{3.5})$ [6], where $c = 6K^2 + 3L^2 + 8K + 3L + 1$ and $v = 3K^2 + L^2 + 2K(N+1) + 2L$ are the numbers of scalar variables and linear/SOC constraints, respectively.

IV. NUMERICAL RESULTS

A. Simulation Setup

We numerically evaluate the performance of the proposed algorithm, with the following settings. The BS located at the cell-center of small-cell serves $L = 4$ UL users and $M = 8$ DL users. All UL users are randomly placed in the cell, while four DL users are randomly placed in zone-1 between 10 and 50 meters, and the other four DL users are randomly located in zone-2 between 50 and 100 meters. The channel vector between BS and user $\mathtt{U} \in \{\mathtt{U}_\ell^{\mathrm{u}}, \mathtt{U}_{ik}^{\mathrm{d}}\}$ is generated as $\mathbf{h} = \sqrt{10^{-\mathrm{PL}_{\mathrm{BS},\mathtt{U}}/10}}\hat{\mathbf{h}}$, with $\mathbf{h} \in \{\mathbf{h}_\ell^{\mathrm{u}}, \mathbf{h}_{ik}^{\mathrm{d}}\}$, while the channel response from $\mathtt{U}_\ell^{\mathrm{u}}$ to $\mathtt{U}_{ik}^{\mathrm{d}}$ is generated as $g_{\ell k} = \sqrt{10^{-\mathrm{PL}_{\ell k}/10}}\hat{g}_{\ell k}$. Here, $\mathrm{PL}_{\mathrm{BS},\mathtt{U}}$ and $\mathrm{PL}_{\ell k}$ represent the path loss (in dB), as given in Table I, with $d_{\mathrm{BS},\mathtt{U}}$ and $d_{\ell k}$ being the distances (in km) between BS and user $\mathtt{U}$ and between users $\mathtt{U}_\ell^{\mathrm{u}}$ and $\mathtt{U}_{ik}^{\mathrm{d}}$, respectively. $\hat{\mathbf{h}}$ and $\hat{g}_{\ell k}$ represent small-scale fading and are distributed as $\mathcal{CN}(\mathbf{0}, \mathbf{I})$. The entries of the SI channel $\mathbf{G}_{\mathrm{SI}}$ are modeled as independent and identically distributed Rician random variables, with the Rician factor of 5 dB [6]. The other parameters are given in Table I, as in [13], [17]. The SRs are divided by $\ln 2$ to be presented in bits/s/Hz. For comparison purpose, the following schemes are also considered: *(i)* Both UL users' decoding order and DL user pairing are randomly selected, referred to as the strategy of random UA (FD-NOMA + RUA); *(ii)* A conventional FD scheme in [7] without applying NOMA is used (FD-Conventional); *(iii)* Under FD-NOMA with RUA, BS serves DL and UL users separately in two independent communication time blocks (HD-NOMA).

TABLE I
SIMULATION PARAMETERS

Parameter	Value
Radius of small cell	100 m
System bandwith, B	10 MHz
Noise power spectral density, $\sigma_{ik}^2 = \sigma_{\mathtt{U}}^2 \equiv \sigma^2$	-174 dBm/Hz
Residual SIS parameter, ρ^2	-90 dB
PL between BS and a user $\mathtt{U}$, $\mathrm{PL}_{\mathrm{BS},\mathtt{U}}$	$103.8 + 20.9\log_{10}(d_{\mathrm{BS},\mathtt{U}})$ dB
PL from $\mathtt{U}_\ell^{\mathrm{u}}$ to $\mathtt{U}_{ik}^{\mathrm{d}}$, $\mathrm{PL}_{\ell k}$	$145.4 + 37.5\log_{10}(d_{\ell k})$ dB
Power budget at UL users, $P_\ell^{\max}, \forall \ell$	18 dBm
Power budget at BS, $P_{\mathrm{bs}}^{\max}$	38 dBm
Number of antennas at BS, N	10
Rate threshold, $\bar{R}_\ell^{\mathrm{u}} = \bar{R}_{ik}^{\mathrm{d}} \equiv \bar{R}, \ \forall \ell, i, k$	1 bps/Hz
Error tolerance, ε	10^{-3}
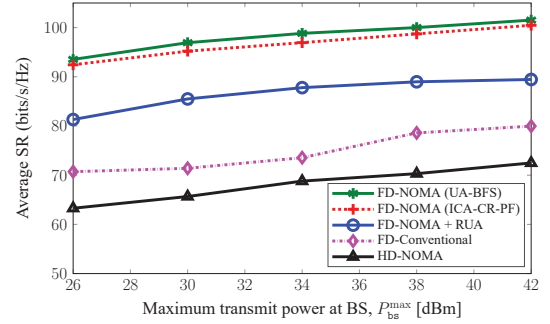
(a) Average SR versus $P_{\mathrm{bs}}^{\max}$.
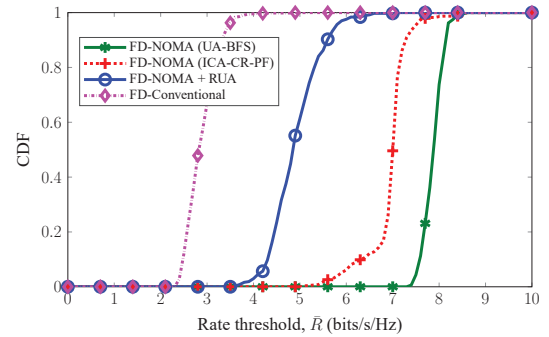

(b) CDF versus the rate threshold.

Fig. 2. System performance for different schemes.

B. Performance Evaluation

Fig. 2 depicts the system performance for different resource allocation schemes, w.r.t. the maximum transmit power at the BS and the minimum rate threshold, respectively. As a benchmark, we implement the brute-force search (BFS) to find the best UA (UA-BFS). As can be seen in Fig. 2(a), the ICA-CR-PF based algorithm deviates only $1\% \sim 2\%$ from the optimal SR, meaning that a very good performance is achieved while with much less complexity compared to the UA-BFS. Fig. 2(b) shows the cumulative distribution function (CDF) of the FD-based schemes as a function of the QoS requirement, $\bar{R}$. The HD-NOMA scheme is omitted here since its DL and UL transmissions are separately executed. Obviously, the probabilities of feasibility of all considered schemes are smaller when $\bar{R}$ is higher. As expected, FD-NOMA schemes can maintain more rate fairness among all DL and UL users when compared with the FD-Conventional scheme. In addition, FD-NOMA schemes using the ICA-CR-PF algorithm offsets about 2 bits/s/Hz of the rate threshold more than the scheme of FD-NOMA with RUA in about 50% of the simulated trials. It further confirms that the joint optimization of UA might help satisfy higher QoS levels for the FD-NOMA schemes.
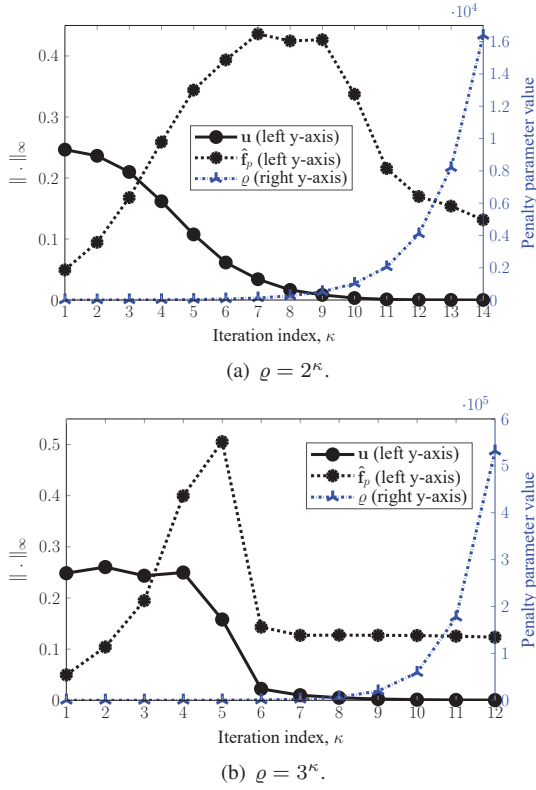
Fig. 3.   Convergence rate of UA variables and PF values with different penalty parameters $\varrho = a^\kappa$, for $a = \{2,3\}$.

C. Convergence Behavior in Different Penalty Parameters

We finally provide further insight into the selection of ϱ in the ICA-CR-PF based algorithm, as illustrated in Fig. 3. In implementation, the penalty parameter $\varrho = a^\kappa$, which increases with the iteration index, provides fast convergence. However, the best value of a mainly depends on the specific setting. Therefore, the ICA-CR-PF based algorithm combined with the binary search is used to find a just once. To evaluate the effectiveness of a, we define the convergence measurements as $\mathbf{u} \triangleq \text{vec}\big([[\alpha_{kj}^2 - \alpha_{kj}]_{k,j \in \mathcal{K}} \ [\beta_{\ell m}^2 - \beta_{\ell m}]_{\ell, m \in \mathcal{L}}]\big)$ and $\hat{\mathbf{f}}_p \triangleq 0.1\text{vec}\big([[f_p(\alpha_{kj})]_{k,j \in \mathcal{K}} \ [f_p(\beta_{\ell m})]_{\ell, m \in \mathcal{L}}]\big)$, where $\text{vec}(\mathbf{X})$ represents the vectorization of matrix $\mathbf{X}$. For example, Fig. 3 depicts the values of $\|\mathbf{u}\|_\infty$ and $\|\hat{\mathbf{f}}_p\|_\infty$ (left y-axis) and penalty parameter ϱ (right y-axis) versus the iteration index κ (common x-axis) in the cases of $a = \{2,3\}$. For the above setting, $a = 3$ in Fig. 3(b) is a better choice as it provides the lower convergence rates of $\|\mathbf{u}\|_\infty$ and $\|\hat{\mathbf{f}}_p\|_\infty$. Remarkably, the convergence behaviors of the UA variables are almost the same for each setting, and thus, the penalty parameter ϱ is determined at the beginning of a setting.

V. CONCLUSION

In this paper, a joint power control and UA problem has been proposed to maximize the sum rate of a cellular FD-NOMA system. A tensor model for DL users and a permutation matrix for UL users have been employed to formulate the UA problem, which significantly reduces the number of association variables. By presenting novel methods to approximate the formulated non-convex problem, an iterative low-complexity algorithm have been developed, which is based

on the ICA framework and PF method. The proposed iterative algorithm improves achievable sum rate at each iteration and converges fast, being also superior to existing algorithms.

APPENDIX A: PROOF OF THEOREM 1

Let $\mathbf{C}_0$ be the unitary matrix representing the clustering indices. It is obvious that $\mathbf{C}_i$, $i \in \mathcal{Z}$, is the change-of-basis matrix of zone i, with respect to the basis $\mathbf{C}_0$. Therefore, $[\mathbf{C}_i]_{kj}$, $k, j \in \mathcal{K}$, with $[\mathbf{X}]_{a,b}$ denoting the element at the a-th row and the b-th column of matrix $\mathbf{X}$, indicates whether the j-th DL user in zone i belongs to the k-th cluster. From **Definition 2**, $\mathbf{C}_1 = \mathbf{C}_0 = \mathbf{I}_K$, leading that a user association matrix $\mathbf{T}^{1i}$ is equivalent to the change-of-basis matrix $\mathbf{C}_i$ w.r.t. the basis $\mathbf{C}_0$. From the transformation law of tensor, the user association matrix $\mathbf{T}^{iz}$, $(i, z) \in \{\mathcal{Z} \times \mathcal{Z}\}$ is calculated by

$$\mathbf{T}^{iz} = \big(\mathbf{T}^{1i}\big)^{-1} \mathbf{C}_1 \mathbf{C}_z = \mathbf{C}_i^{-1} \mathbf{C}_z. \tag{A.1}$$

Based on **Definition 1**, the matrix $\mathbf{C}_i$, $i \in \mathcal{Z}$, satisfies the following conditions: $\sum_{k \in \mathcal{K}} [\mathbf{C}_i]_{kj} = 1$ and $\sum_{j \in \mathcal{K}} [\mathbf{C}_i]_{kj} = 1$. Accordingly, $\mathbf{C}_i$ characterized as a permutation matrix, satisfies the property that $\mathbf{C}_i^{-1} = \mathbf{C}_i^T$. Equation (1) is then obtained by substituting $\mathbf{C}_i^{-1} = \mathbf{C}_i^T$ into (A.1).

REFERENCES

[1] J. Andrews *et al.*, "What will 5G be?" *IEEE J. Select. Area Commun.*, vol. 32, no. 6, pp. 1065–1082, June 2014.
[2] Z. Ding, Y. Liu, J. Choi, Q. Sun, M. Elkashlan, C. L. I, and H. V. Poor, "Application of non-orthogonal multiple access in LTE and 5G networks," *IEEE Commun. Mag.*, vol. 55, no. 2, pp. 185–191, Feb. 2017.
[3] S. M. R. Islam *et al.*, "Power-domain non-orthogonal multiple access (NOMA) in 5G systems: Potentials and challenges," *IEEE Commun. Surveys Tutor.*, vol. 19, no. 2, pp. 721–742, Second quarter 2017.
[4] A. Yadav *et al.*, "Full-duplex communications: Performance in ultradense mm-wave small-cell wireless networks," *IEEE Veh. Technol. Mag.*, vol. 13, no. 2, pp. 40–47, June 2018.
[5] Z. Ding *et al.*, "On the coexistence between full-duplex and NOMA," *IEEE Wireless Commun. Lett.*, vol. 7, no. 5, pp. 692–695, Oct. 2018.
[6] V.-D. Nguyen, H. V. Nguyen, O. A. Dobre, and O.-S. Shin, "A new design paradigm for secure full-duplex multiuser systems," *IEEE J. Select. Areas Commun.*, vol. 36, no. 7, pp. 1480–1498, July 2018.
[7] D. Nguyen, L.-N. Tran, P. Pirinen, and M. Latva-aho, "On the spectral efficiency of full-duplex small cell wireless systems," *IEEE Trans. Wireless Commun.*, vol. 13, no. 9, pp. 4896–4910, Sept. 2014.
[8] V.-D. Nguyen *et al.*, "Spectral efficiency of full-duplex multiuser system: Beamforming design, user grouping, and time allocation," *IEEE Access*, vol. 5, pp. 5785–5797, Mar. 2017.
[9] A. Yadav *et al.*, "Energy and traffic aware full duplex communications for 5G systems," *IEEE Access*, vol. 5, pp. 11278–11290, May 2017.
[10] V.-P. Bui *et al.*, "Optimal user pairing for achieving rate fairness in downlink NOMA networks," in *Inter. Conf. Artificial Intelligence Inform. Commun. (ICAIIC)*, Feb. 2019, pp. 575–578.
[11] Y. Sun *et al.*, "Optimal joint power and subcarrier allocation for full-duplex multicarrier non-orthogonal multiple access systems," *IEEE Trans. Commun.*, vol. 65, no. 3, pp. 1077–1091, Mar. 2017.
[12] H. V. Nguyen *et al.*, "Joint NOMA beamforming and user scheduling for sum rate maximization in a full-duplex system," in *Proc. Inter. Conf. Inform. Commun. Technol. Converg. (ICTC)*, Oct. 2017, pp. 731–733.
[13] D. Bharadia *et al.*, "Full duplex radios," in *Proc. ACM SIGCOMM Computer Commun. Review*, vol. 43, no. 4, 2013, pp. 375–386.
[14] D. Tse and P. Viswanath, *Fundamentals of Wireless Communication*. Cambridge Univ. Press, UK, 2005.
[15] V.-D. Nguyen *et al.*, "Precoder design for signal superposition in MIMO-NOMA multicell networks," *IEEE J. Select. Areas Commun.*, vol. 35, no. 12, pp. 2681–2695, Dec. 2017.
[16] Z. Ding *et al.*, "A general MIMO framework for NOMA downlink and uplink transmission based on signal alignment," *IEEE Trans. Wireless Commun.*, vol. 15, no. 6, pp. 4483–4454, June 2016.
[17] *3GPP Technical Specification Group Radio Access Network, Evolved Universal Terrestrial Radio Access (E-UTRA): Further Advancements for E-UTRA Physical Layer Aspects (Release 9)*, document 3GPP TS 36.814 V9.0.0, 2010.